

In vivo femtosecond endosurgery: an intestinal epithelial regeneration-after-injury model

Myunghwan Choi and Seok Hyun Yun*

Harvard Medical School and Wellman Center for Photomedicine, Massachusetts General Hospital, 65 Landsdowne Street, Cambridge, Massachusetts 02139, USA
*syun@hms.harvard.edu

Abstract: Regeneration of the intestinal epithelium after injury or during pathogenesis is a dynamic cellular process critical for host immunity. However, current epithelial injury models provide poor spatial control, complicating the study of precise cellular responses. Here we developed endoscopic femtosecond-laser surgery capable of generating acute tissue injury. A side-view probe provides a convenient access to the distal colon in the mouse *in vivo* and allows real-time intraoperative monitoring as well as pre- and post-surgery examinations via multiphoton imaging. The photo-induced damage showed a nonlinear dependence on laser intensity. At an optical power of 200 mW (2.5 nJ per pulse), scanning the beam focus over 300x300 μm^2 area in the colonic mucosa generated substantial vascular damages within 30 s. We confirmed the localized tissue damage and the physiologic regeneration of the disrupted epithelium by *in situ* barrier function assays, validating the animal model for epithelial regeneration following injury. The femtosecond endosurgery technique is applicable to various experimental models based on laser-induced perturbations.

©2013 Optical Society of America

OCIS codes: (170.2150) Endoscopic imaging; (180.4315) Nonlinear microscopy; (170.1020) Ablation of tissue; (000.1430) Biology and medicine.

References and links

1. H. Sokol, K. L. Conway, M. Zhang, M. Choi, B. Morin, Z. Cao, E. J. Villablanca, C. Li, C. Wijemanga, S. H. Yun, H. N. Shi, and R. J. Xavier, "Card9 mediates intestinal epithelial cell restitution, T-helper 17 responses, and control of bacterial infection in mice," *Gastroenterology* **145**, 591–601 (2013).
2. M. R. Walker, K. K. Patel, and T. S. Stappenbeck, "The stem cell niche," *J. Pathol.* **217**(2), 169–180 (2009).
3. T. Sato, R. G. Vries, H. J. Snippert, M. van de Wetering, N. Barker, D. E. Stange, J. H. van Es, A. Abo, P. Kujala, P. J. Peters, and H. Clevers, "Single Lgr5 stem cells build crypt-villus structures *in vitro* without a mesenchymal niche," *Nature* **459**(7244), 262–265 (2009).
4. H. Miyoshi, R. Ajima, C. T. Luo, T. P. Yamaguchi, and T. S. Stappenbeck, "Wnt5a potentiates TGF- β signaling to promote colonic crypt regeneration after tissue injury," *Science* **338**(6103), 108–113 (2012).
5. L. Li and H. Clevers, "Coexistence of quiescent and active adult stem cells in mammals," *Science* **327**(5965), 542–545 (2010).
6. S. Wirtz, C. Neufert, B. Weigmann, and M. F. Neurath, "Chemically induced mouse models of intestinal inflammation," *Nat. Protoc.* **2**(3), 541–546 (2007).
7. W. Strober, I. J. Fuss, and R. S. Blumberg, "The immunology of mucosal models of inflammation," *Annu. Rev. Immunol.* **20**(1), 495–549 (2002).
8. H. Seno, H. Miyoshi, S. L. Brown, M. J. Geske, M. Colonna, and T. S. Stappenbeck, "Efficient colonic mucosal wound repair requires Trem2 signaling," *Proc. Natl. Acad. Sci. U. S. A.* **106**(1), 256–261 (2009).
9. W. R. Zipfel, R. M. Williams, and W. W. Webb, "Nonlinear magic: multiphoton microscopy in the biosciences," *Nat. Biotechnol.* **21**(11), 1369–1377 (2003).
10. M. Antkowiak, M. L. Torres-Mapa, K. Dholakia, and F. J. Gunn-Moore, "Quantitative phase study of the dynamic cellular response in femtosecond laser photoporation," *Biomed. Opt. Express* **1**(2), 414–424 (2010).
11. W. Watanabe, N. Arakawa, S. Matsunaga, T. Higashi, K. Fukui, K. Isobe, and K. Itoh, "Femtosecond laser disruption of subcellular organelles in a living cell," *Opt. Express* **12**(18), 4203–4213 (2004).
12. N. Nishimura, C. B. Schaffer, B. Friedman, P. S. Tsai, P. D. Lyden, and D. Kleinfeld, "Targeted insult to subsurface cortical blood vessels using ultrashort laser pulses: three models of stroke," *Nat. Methods* **3**(2), 99–108 (2006).

13. M. Choi, T. Ku, K. Chong, J. Yoon, and C. Choi, "Minimally invasive molecular delivery into the brain using optical modulation of vascular permeability," *Proc. Natl. Acad. Sci. U. S. A.* **108**(22), 9256–9261 (2011).
14. M. Choi, J. Yoon, and C. Choi, "Label-free optical control of arterial contraction," *J. Biomed. Opt.* **15**(1), 015006 (2010).
15. M. Q. Salomão and S. E. Wilson, "Femtosecond laser in situ keratomileusis," *J. Cataract Refract. Surg.* **36**(6), 1024–1032 (2010).
16. J. K. Kim, W. M. Lee, P. Kim, M. Choi, K. Jung, S. Kim, and S. H. Yun, "Fabrication and operation of GRIN probes for in vivo fluorescence cellular imaging of internal organs in small animals," *Nat. Protoc.* **7**(8), 1456–1469 (2012).
17. V. K. Sidhaye, K. S. Schweitzer, M. J. Caterina, L. Shimoda, and L. S. King, "Shear stress regulates aquaporin-5 and airway epithelial barrier function," *Proc. Natl. Acad. Sci. U. S. A.* **105**(9), 3345–3350 (2008).
18. P. Kim, E. Chung, H. Yamashita, K. E. Hung, A. Mizoguchi, R. Kucherlapati, D. Fukumura, R. K. Jain, and S. H. Yun, "In vivo wide-area cellular imaging by side-view endomicroscopy," *Nat. Methods* **7**(4), 303–305 (2010).
19. A. Vogel, J. Noack, G. Hüttman, and G. Paltauf, "Mechanisms of femtosecond laser nanosurgery of cells and tissues," *Appl. Phys. B* **81**(8), 1015–1047 (2005).
20. C. B. Schaffner, A. Brodeur, J. F. García, and E. Mazur, "Micromachining bulk glass by use of femtosecond laser pulses with nanojoule energy," *Opt. Lett.* **26**(2), 93–95 (2001).
21. A. Y. Shih, P. Blinder, P. S. Tsai, B. Friedman, G. Stanley, P. D. Lyden, and D. Kleinfeld, "The smallest stroke: occlusion of one penetrating vessel leads to infarction and a cognitive deficit," *Nat. Neurosci.* **16**(1), 55–63 (2013).

1. Introduction

The intestinal epithelium plays a critical role in innate immunity by providing the physiologic barrier between the host tissue and the luminal environment [1]. The protective barrier is constantly challenged by pathogens and toxins in the intestine and often disrupted by serious pathologic conditions, such as injury, infection, and inflammation [2]. During normal homeostasis, the epithelium of mammalian intestine is replenished continuously at a turnover rate of 3-5 days [3]. However, this process can also be affected during pathogenesis, impeding healing. Understanding the detailed processes involved in the epithelial regeneration is an active area of research in the studies of intestinal diseases [4,5].

To study the epithelial regeneration, several experimental models have been developed. The current gold standard is murine models based on intestinal injury. In these models, toxic chemicals, such as dextran sodium sulfate (DSS), are introduced to the mouse, which results in the disruption of intestinal epithelium [6]. Alternatively, several genetically modified mice, such as interleukin-10 knockout mice, are widely used [7]. Although these models can effectively induce severe tissue injury, the location and timing of the injury cannot be precisely controlled, which causes undesirable uncertainties in the study of regeneration. To overcome this limitation, a focal mechanical injury model through biopsy forceps has been developed [8]. However, the control of the size and degree of injury is difficult, and the minimum size of injury is limited to about 1 mm².

Femtosecond pulsed lasers can generate tightly localized injury in three dimensions through nonlinear absorption [9]. This technique has been used to ablate individual intracellular compartments, such as plasma membrane [10], chromosome, and mitochondrion in cultured mammalian cells [11]. In experimental animals, femtosecond laser surgery has been used to create micro-thrombi [12], deliver drugs [13], and control vascular tones [14]. Femtosecond laser is widely used in precision refractive surgery in the clinic [15].

Here, we describe a novel endoscopic microsurgery technique for generating tissue injury in the murine colon with high spatial and temporal precision. We use a side-view optical probe integrated into a video-rate multiphoton microscope [16] to deliver focused femtosecond pulses while simultaneously visualizing the colon tissue at cellular resolution in real time. We test and validate this technique by monitoring and quantifying the laser-induced tissue damage and the subsequent regeneration of the epithelium.

2. Method and results

2.1 Multiphoton imaging system and a side-view surgery probe

We used a home-built multiphoton microscope for image-guided endosurgery (Fig. 1(a)). The light source was a mode-locked Ti:Sapphire laser (MaiTai DeepSee eHP, Newport) delivering 80-MHz 120-fs pulses at 690-1040 nm. In all experiments here, the laser was tuned to 800 nm. A prism-pair pulse chirper compensated the positive chromatic material dispersion in the side-view probe as well as other lenses in the beam path. The optical power was adjusted by using a rotating half-wave plate and a polarizing beam splitter. A polygon mirror and a galvanometer-mounted mirror were used for beam scanning at a frame rate of 30 Hz. The side-view probe was fabricated with a graded-index doublet comprising a 0.18-NA relay lens and 0.5-NA focusing lens (Grintech) and a 90-degree prism mirror [17]. The length and diameter of the probe, including a protective metal sleeve, was approximately 56 mm and 1.25 mm, respectively. The probe was mounted on a custom-made translation/rotation stage with its proximal surface aligned to the focal plane of a 10X objective lens (0.25 NA, Olympus). The effective NA of the probe was about 0.35, resulting in the transverse and axial resolution (full-width-at-half-maxima: FWHM) of 1 and 10 μm , respectively. Nonlinear laser-induced damage occurs at (or near) the focus of the laser beam. The beam focus was scanned laterally in the raster pattern over a field-of-view (FOV) of $300 \times 300 \mu\text{m}^2$ (Fig. 1(b)), allowing real-time imaging of the tissue, although in principle the beam focus could be held stationary during surgery. Pre and post-op imaging was done at significantly lower laser power to avoid tissue damage. The working distance was tunable over a few hundreds micrometers by adjusting the distance between the probe and the microscope objective lens.

For animal experiments, we used C57BL/6J mice (7-10 weeks, female, Jackson Laboratory). The procedure for mouse colon imaging has been described previously [16]. Mice were anesthetized by intraperitoneal injection of ketamine (90 mg/kg) and xylazine (9 mg/kg) in phosphate buffered saline (PBS). The entire distal colon of a mouse can be accessed by rotating the probe and moving an animal stage [18]. All animal experiments were approved by the Institutional Animal Care and Use Committee at the Massachusetts General Hospital.

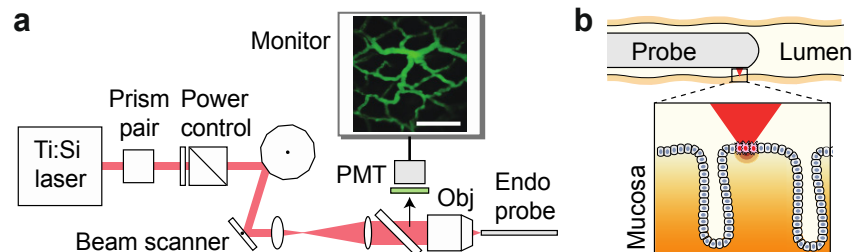


Fig. 1. (a) A schematic of the multiphoton imaging and endosurgery system. Two-photon fluorescence images are displayed in a monitor in real time at 30 frames per second. The typical laser power at the tissue was adjusted to be 20-40 mW (i.e. 0.25-0.5 nJ) for noninvasive imaging and increased to 200 mW (i.e. 2.5 nJ) for inducing tissue damage. Displayed in the monitor in this illustration is a fluorescence image of the typical blood vessels in the colonic mucosa of a mouse. Scale bar, 100 μm . (b) Illustration of femtosecond laser endosurgery in the colon by the side-view probe.

2.2 Laser-induced damage of blood vessels in vivo

Among various options for labeling the colon wall for *in vivo* imaging, we used an intravascular dye, fluorescein-conjugated dextran (molecular weight: 2 MDa), to visualize and assess the laser-induced damage on the blood vessels in the mucosa. The dye was injected into the mouse intravenously and imaged by using two-photon excitation at 800 nm at an average power of 20-40 mW. The probe was located at a specific region in the distal colon,

delivering the raster-scanned laser beam over a $300 \times 300 \mu\text{m}^2$ area. The focal plane was set within the superficial mucosa layer, approximately $20 \mu\text{m}$ deep from the surface. At the lower power level, we observed no sign of damage to the blood vessels during imaging for longer than 10 min. Even when the laser power was increased to 100 mW, we did not detect any noticeable changes in the blood flow or leakage of the dye for exposure duration of up to 60 s. However, when the laser power was increased to 200 mW measured at the exit of the probe, two distinctive changes in vascular dynamics occurred (Fig. 2(a) and Media 1). First, the intravascular dye molecules extravasated, diffused out, and filled the inter-crypt region. The leakage is a prominent indicator of vascular damage. Second, the intravascular thrombi were formed, as identified by the appearance of dark particles in the vascular lumen, which interrupted or completely blocked the blood flows depending on their sizes (Fig. 2(b)). The progression of the vascular changes reached a steady state in 60 s.

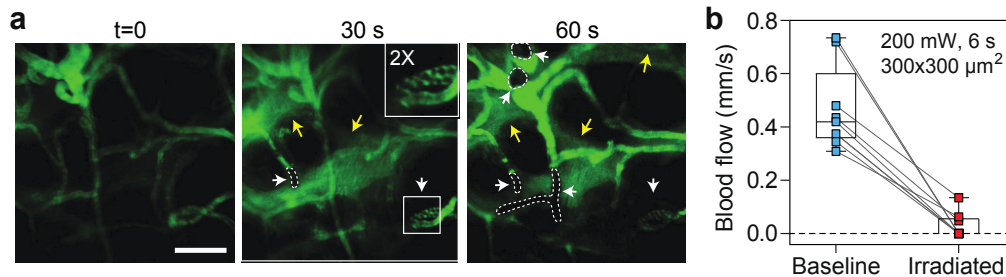


Fig. 2. Laser-induced damage on the mucosal blood vessels. (a) Time-series vascular images during femtosecond endosurgery (Media 1, 5.5 MB). Note that formation of intravascular clots (white arrows) and leakage of the vascular dye (yellow arrows). Scale bar, $50 \mu\text{m}$. (b) Quantification of the blood flow before and after the laser irradiation in (a).

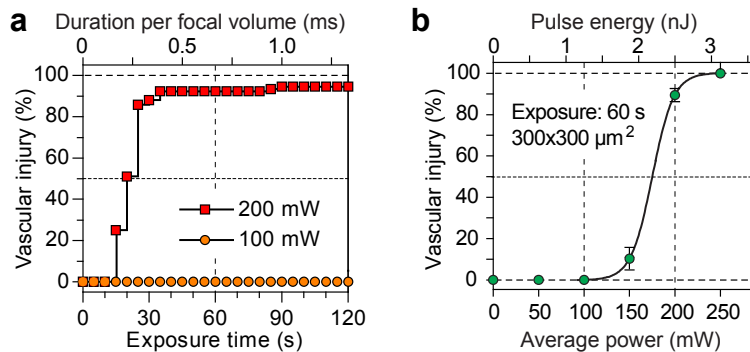


Fig. 3. Power dependence of the laser-induced tissue injury. (a) The percentage of non-functional vascular segments in the FOV ($300 \times 300 \mu\text{m}^2$) for 100 mW and 200 mW, measured at 5 sec interval ($n = 75-92$). (b) The percentage of non-functional vascular segments after exposure for 60 s ($n = 8$). Over 60 s, the effective irradiation time on each focal point ($1 \mu\text{m}^2$) is just 0.67 ms. Line, a Sigmoidal curve fit ($R^2 = 0.97$).

Using the method described above, we investigated the degree of vascular injury at various irradiation conditions. First, we quantified the dependency of vascular injury on exposure time at two power levels of 100 mW and 200 mW, respectively (Fig. 3(a)). At 100 mW, no vascular segments ($n = 75$) showed any sign of injury. At 200 mW, thrombosis and plasma leakage were apparent after 10 s and rapidly progressed until 25 s with time to half-maximal damage of 20 s ($n = 92$). Considering the laser scanning, this duration corresponds to an effective exposure time of ~ 0.2 ms per focal volume. Next, for various laser powers from 0 to 250 mW at the same exposure time of 60 s, we measured the number of vascular segments with disrupted blood flows. The result showed a sigmoidal dependence of the injury on the laser power (Fig. 3(b)). No damage occurred up to 100 mW and a complete

damage was observed at 250 mW. The power for half-maximal damage (ED_{50}) was 175 mW. At this level, the pulse energy is about 2.2 nJ per pulse (at 80 MHz), the peak intensity at the focus ($1 \mu\text{m}^2$) is about 10^{12} W/cm^2 , and the total fluence integrated over 60 s is $0.11 \text{ mJ}/\mu\text{m}^2$. These results indicate that the mechanism of injury is a multiphoton process presumably involving nonlinear absorption.

2.3 Characterization of the laser-induced damage of the colonic epithelium

To characterize the laser-induced cell death, we developed two different assay protocols that stain the colon *in vivo* and examine the tissue *ex vivo*. The tissue damage was induced over an extensive area in the colon by continuously translating the probe along the lumen (by moving the mouse) over 2 mm. First, we used a cell-death probe, Ethidium homodimer (Life Technologies), which is a fluorescent DNA-staining dye that is impermeable to viable cellular membranes but able to stain the nuclei of dead cells with damaged membranes. The focal plane of the surgical beam was set to target the epithelium. Post endosurgery, a solution of Ethidium homodimer (100 nM, 0.5 ml) was injected into the colon. After 3-min incubation, the remaining dye was flushed out with warm PBS. The colon tissue was then excised from the sacrificed mouse and examined under a wide-field microscope. The damaged region was readily identified by the disrupted crypt structure in the bright-field images (Fig. 4(a)). The injured area overlapped with the red fluorescence region, confirming the significant necrotic cell death in the irradiated region (Fig. 4(b)). The width of the stained area was about $500 \mu\text{m}$, larger than $300 \mu\text{m}$ expected from the FOV, which is presumably due to the physiologic tissue motion during irradiation.

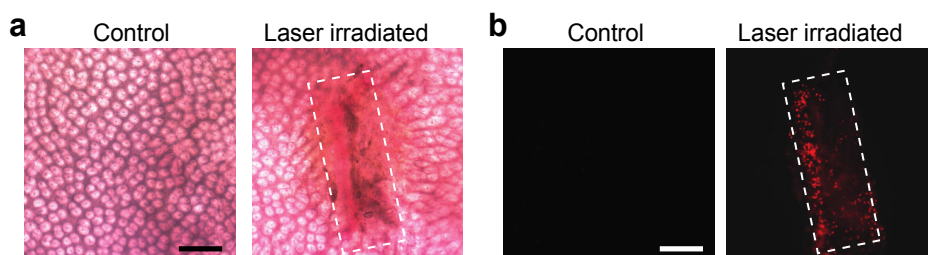


Fig. 4. Laser-induced cell death. (a) Bright-field images of excised tissues. (b) Fluorescence images of the tissues. Dead cells are identified by red fluorescence from Ethidium homodimer. The white dotted rectangle corresponds to the elongated irradiation region achieved by translating the probe along the lumen. Scale bars, $500 \mu\text{m}$.

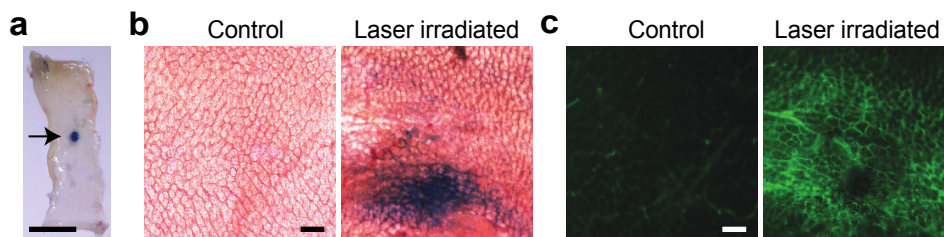


Fig. 5. Evaluation of the epithelial barrier function. (a) A photograph showing Evans blue in the laser-irradiated region (arrow). (b) Bright-field images of the intact (control) and laser-injured (irradiated) areas. (c) Fluorescence (fluorescein-conjugated dextran) images of the intact and irradiated areas. Scale bars, 5 mm in (a) and $500 \mu\text{m}$ in (b-c).

Second, we used another membrane impermeable dye, Evans blue, to evaluate the barrier function of the epithelium [17]. After flushing Evans blue (1% w/v, 0.5 ml; Sigma Aldrich) in the colon *in vivo* for 3 min, the mouse was sacrificed, and the colon tissues were excised. We readily observed blue stain at the laser-irradiated area (Fig. 5(a)), indicating that femtosecond endosurgery effectively damaged the physiologic epithelial barrier. The stained areas were

typically larger than the irradiated area, presumably due to diffusion of the permeated dye in the tissue or secondary ischemic injury by disrupted blood flow. In magnified view, the laser-injured area was also noticeable by the retention of leaked dextran-conjugated vascular dyes (Figs. 5(b) and 5(c)). The dye retention persisted over a week. This allowed us to find the injury site at multiple time points, particularly useful for studying time-lapse epithelial regeneration.

We tested the feasibility of longitudinal imaging of the injured site *in vivo* (Fig. 6). At 2 days after endosurgery, we imaged the mouse using the same probe. The injury site was easily identified by the prominent retention of the leaked vascular dye that had been injected at Day 0 prior to endosurgery. Further *in situ* staining with Evans Blue (red fluorescence) at Day 2 visualized the compromised epithelial barrier function of the injured region.

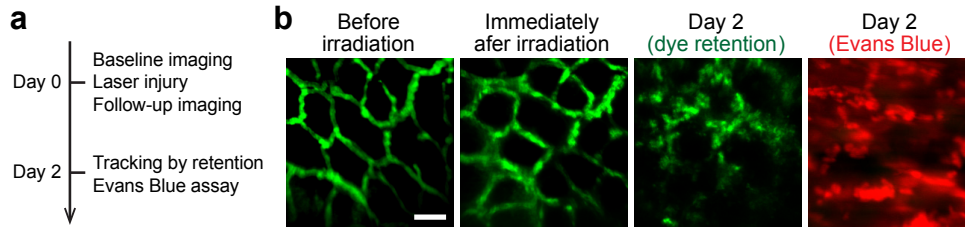


Fig. 6. Longitudinal follow-up imaging *in vivo*. (a) Experimental design. (b) Images acquired from a mouse at pre-op, post-op, and 2 days after the laser injury. Scale bar, 50 μm .

2.4 Regeneration of the damaged epithelium

Having confirmed the laser-induced damage, we investigated the regeneration of the damaged epithelium. We induced tissue injury over a fixed area and performed the barrier function assay at days 0, 1, and 4, respectively ($n = 9$ mice; $n = 3$ for each time point). We measured the area of the tissue stained by Evans blue as a metric to quantify the extent of the disruption of the barrier function. We found that the barrier function recovered significantly within 1 day and restored completely in 4 days (Fig. 7). This rapid regeneration is consistent with the reported regeneration kinetics with full thickness mucosal biopsy injury [8]. The normal regeneration after laser injury indicates that femtosecond endosurgery can induce physiologically relevant injury.

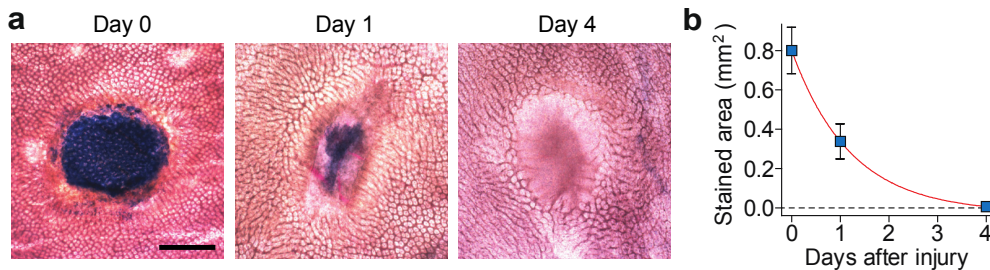


Fig. 7. Epithelial regeneration after laser-induced injury. (a) Bright-field images taken with *ex vivo* preparation at 0, 1, and 4 days after laser endosurgery. The penetration of Evans blue indicates the disruption of the epithelial barrier function. Scale bar, 500 μm . (b) The measured tissue area stained by Evans blue. Error bars, standard deviations ($n = 3$).

3. Discussion

We have developed a novel imaged-guided laser surgery technique and applied it for inducing epithelial tissue injury in the murine colon *in vivo*. Compared to the previous chemical and mechanical injury models, the optical method offers much higher spatial precision and, in principle, allows the degree of injury to be controlled by the irradiation power and duration. In this work, the laser focus was raster-scanned to induce tissue injury at a sub-millimeter

scale. Single cell-level injury might be possible by short irradiation without scanning. A practical bottleneck limiting the spatial precision is the tissue movement caused by heart beating and breathing. Gentle pressure to the tissue by the probe tip could suppress the vertical movement of tissue, but the residual lateral movement limits spatial precision and blurs the margin of injury. A potential solution is to gate the surgery beam based on real-time images.

We observed a comprehensive disruption of the superficial blood vessels in the mucosa within 10-60 s at a power of 200-250 mW (80-MHz, 800 nm). The corresponding pulse energy of about 3 nJ is an order of magnitude lower than the previously reported threshold for inducing stroke in the brain through photo-mechanical effect (i.e. optical breakdown) [12]. The extent of vascular injury was nonlinearly dependent on the power level, and the damage progressed with a relatively sharp onset at about 0.2 ms exposure per focal volume at 200 mW. The nonlinear damage threshold suggests that the primary mechanism of tissue injury is through photochemical effects (i.e. low-density plasma formation) by multiphoton absorption, but some contribution of thermal injury is also expected [19]. Optical probes with higher NA may lower the threshold power by enhancing plasma formation [20]. Besides the epithelium and superficial mucosa, it might be possible to induce tissue damage in the deeper mucosal layer by increasing the NA of the probe and optimizing the laser wavelength.

We used Evans Blue to measure the epithelial barrier function and its recovery. The Evans Blue staining exhibited an area extended about 200 μm outside the actual laser-irradiated region (Fig. 7(a)). This may be attributed largely to two factors. First, vascular thrombosis might result in ischemic tissue injury in the surrounding area; such phenomenon has been observed when a single 0.1 μJ pulse was delivered on a penetrating arteriole in the brain cortex [21]. Secondly, Evans blue penetrated into the mucosa might diffuse laterally to the neighboring tissue underneath undisrupted epithelium.

The femtosecond-induced mouse model presented here has recently been applied to investigating the role of Card9 gene in epithelial restitution during inflammatory immune response [1]. In this study, the femtosecond endosurgery enabled regeneration-after-injury assay of the colonic epithelium in response to the genetic intervention on Card9 gene. The endosurgery technique can be extended to other tissues in various parts in the body [16] to generate photo-induced perturbations such as tissue injury, enhanced permeability, and cell activation [12–14]. Image-guided femtosecond laser endosurgery is expected to be useful in a wide range of applications.

Acknowledgments

We acknowledge Ramik Xavier, Kara Conway and Eduardo Villablanca for motivating this work and Alfred Vogel for helpful discussion. This work was supported by grants from National Institutes of Health (U54CA143837, P41EB015903, P01CA080124).